

行政院國家科學委員會專題研究計畫 成果報告

錳離子增強與擴散磁振造影於大腦功能與軸突纖維束可塑性之研究

研究成果報告(精簡版)

計畫類別：個別型
計畫編號：NSC 99-2314-B-040-001-
執行期間：99年05月01日至100年07月31日
執行單位：中山醫學大學醫學影像暨放射科學系

計畫主持人：翁駿程

計畫參與人員：碩士班研究生-兼任助理人員：彭逸玫
碩士班研究生-兼任助理人員：謝政學
碩士班研究生-兼任助理人員：賴柏宏

報告附件：出席國際會議研究心得報告及發表論文

處理方式：本計畫可公開查詢

中華民國 100 年 10 月 27 日

行政院國家科學委員會補助專題研究計畫 成果報告
 期中進度報告

錳離子增強與擴散磁振造影於大腦功能與軸突纖維束可塑性之研究

Mapping plasticity of cerebral activity and axonal fiber tract using manganese
enhanced and diffusion magnetic resonance imaging

計畫類別：個別型計畫 整合型計畫

計畫編號：NSC99-2314-B-040-001

執行期間：99年5月1日至100年7月31日

執行機構及系所：中山醫學大學醫學影像暨放射科學系

計畫主持人：翁駿程

共同主持人：

計畫參與人員：彭逸玟、謝政學、賴柏宏

成果報告類型(依經費核定清單規定繳交)：精簡報告 完整報告

本計畫除繳交成果報告外，另須繳交以下出國心得報告：

赴國外出差或研習心得報告

赴大陸地區出差或研習心得報告

出席國際學術會議心得報告

國際合作研究計畫國外研究報告

處理方式：除列管計畫及下列情形者外，得立即公開查詢

涉及專利或其他智慧財產權，一年二年後可公開查詢

中 華 民 國 100 年 7 月 31 日

中文摘要及關鍵詞

腦是由一簡單的管狀結構發展至非常複雜的組織。了解腦在不同階段的解剖特徵，不僅可對發育過程進一步的認識，也有助於探討腦部的相關異常和疾病。大鼠初級觸覺皮層桶狀區的神經拓撲分佈，是研究神經功能與可塑性的最佳模型，然而以高空間解析度與精準空間定位方法，非侵入式地造影大腦結構發育、功能與可塑性仍具有很高的挑戰性。本計畫的目標為發展新的造影方法來偵測大腦結構與功能的進行，包括發育、神經活化、以及神經可塑性。我們嘗試以擴散張量磁振造影與錳離子增強磁振造影，建立大白兔大腦發育與大鼠於鬍鬚刺激下，造影大腦皮質之適宜的工作平台；我們也嘗試以功能性磁振造影術，建立了大鼠於手指刺激下，造影出大腦手指初級觸覺皮質區，並應用至斷指大鼠大腦可塑性之研究。我們發展及改良了擴散張量磁振造影、功能性磁振造影與錳離子增強磁振造影技術，能以最低侵入程度來研究大腦結構與功能，此外這個研究使我們更加理解對所發展的大腦造影術的應用範圍。

我們以擴散張量影像的方式來收集資料並分析活體兔腦(4週至40週)，藉由追蹤大腦內較具代表性的白質神經纖維如嗅球路徑、胼胝體和海馬迴，非等張性、平均擴散係數、R2值的數據來比較不同時間的發育情形。並合併神經追蹤術，以呈現出不同時間點的白質神經纖維，以及大腦灰質、全腦等不同區域的神經束圖及體積分析。結果顯示，R2值和擴散非等張性隨著年齡增加而增加；相對地，平均擴散係數隨著年齡增加而減少。神經追蹤術對於所有追蹤區域，皆呈現出隨著成熟兔腦而趨於完整的神經顯微結構。我們以錳離子增強磁振造影術所造影大鼠大腦鬍鬚皮質區，證實了大腦中錳離子增強皮質區域與鬍鬚觸覺誘發神經活化間的關係，在大腦皮質反應區，鬍鬚刺激組的大鼠之影像強度(1.72 ± 0.22)與R1值(1.12 ± 0.16)皆比控制組的值高(1.27 ± 0.14 , $p < 0.05$; 0.83 ± 0.21 , $p < 0.05$)。我們也證實了在11.7 T的高場下，以功能性磁振造影術可以造影出單一手指觸覺皮質區，及斷指大鼠的大腦皮質可塑性。二根手指反應區質心的距離由控制組的 1.45 ± 0.29 mm 下降至斷指組的 0.90 ± 0.21 mm ($p < 0.01$)。這個技術對於研究大鼠的神經可塑性有很大的幫助。

總結而言，我們成功的使用擴散張量磁振造影與錳離子增強磁振造影的策略，以非侵入性的方式及技術，造影出大白兔大腦發育與大鼠大腦神經活化；並且配合被我們完整建立的全腦功能性磁振造影，我們以非侵入性的方式得到更多過去必須以侵入性的組織切片或耗時的電生理量測所取得的資訊。據我們的瞭解，這是世界上首次以功能性磁振造影術來研究大腦皮質神經桶的可塑性。未來這些發展於小動物上的磁振造影術將可以推展至人的研究與應用上，而這些新造影術的發展將有助於正常大腦以及因為學習、可塑性、藥物或基因調控而變化大腦的研究。

關鍵字：擴散張量磁振造影、錳離子增強磁振造影、功能性磁振造影、大腦發育、神經活化、神經塑化、初級觸覺皮質區、皮層桶狀區。

英文摘要及關鍵詞

The brain is extraordinarily complex, and yet its origin is a simple tubular structure. Characterizing its anatomy at different stages of brain development not only aids in understanding this highly ordered process but also provides clues to detecting abnormalities caused by genetic or environmental factors. The topographic organization of cortical barrel in layer IV of rat primary somatosensory cortex is a good model for studying neural function and plasticity. However, mapping brain development, function and plasticity with high spatial resolution and accurate spatial localization methods non-invasively remained challenges. The overall objectives of this project were to develop novel imaging techniques to monitor structural and functional processes of the brain, including development, neural activity, and neural plasticity. We sought to establish a feasible working protocol of applying diffusion tensor imaging (DTI) and manganese-enhanced magnetic resonance imaging (MEMRI) to map the white matter development of rabbit brain and cortical barrels of the rat following whisker stimulation. We'd also like to test the feasibility of using functional MRI (fMRI) to map the forepaw digit representations in the primary somatosensory cortex of the rat and to apply to the study of cortical plasticity after digit amputation. The development of these technologies provided three techniques, i.e. fMRI, MEMRI and DTI, these can be used to study brain function and structure in minimally invasive ways. In addition, the study allowed us to better understand the range of applicability of new brain imaging techniques that were developed.

Our results showed that color maps of diffusion indices, R2 mapping, and 3D tractography revealed that important white matter tracts of rabbit brain, such as the olfactory tract, corpus callosum and hippocampus, become apparent during mature period. Regional DTI tractography of the white matter tracts showed refinement in regional tract architecture with maturation. The white matter anisotropy and R2 values increased with age, and the diffusion coefficient decreased with age. We have mapped rat whisker barrels using the MEMRI method and have shown a clear relationship between manganese-enhanced cortical regions and whisker tactile-sense-evoked activity. In the right cortical barrels, the enhancement ratios (1.72 ± 0.22) and R1 values (1.12 ± 0.16) in the whisker stimulation group were significantly higher than those (1.27 ± 0.14 , $p < 0.05$; 0.83 ± 0.21 , $p < 0.05$) in the control group. We have also demonstrated that forepaw barrel subfields of single digits can be reliably mapped using fMRI at high field. The alteration of the digit representation after digit amputation was also detected. The distance between the centers of mass of two digits representations decreased from 1.45 ± 0.29 mm in the control group to 0.90 ± 0.21 mm ($p < 0.01$) in the amputated group. The method will be useful to study neural plasticity in rat brains after surgical or genetic manipulation.

In conclusions, exciting DTI and MEMRI strategies showed great promise for enabling non-invasive techniques to map neuroarchitecture and neuronal activity throughout the animal brain non-invasively. Combined with established whole brain fMRI techniques, it became possible to get an increasing range of information non-invasively that in the past required invasive histology or time consuming electrophysiology. To the best of our knowledge this is the first fMRI demonstration of plasticity in cortical columns by fMRI. In the future, these MRI techniques developed in animals can often be extended for use in humans. The development of these new imaging techniques will be used to study the normal rodent brain and changes in the brain that occur during learning and plasticity or due to specific genetic changes.

Keywords: diffusion tensor imaging, manganese-enhanced MRI, functional MRI, brain development, neural activity, neural plasticity, primary somatosensory cortex, cortical barrels.

報告內容

前言

Brain is a wondrous and complex organic computer that governs every motion of our bodies. Within this computer there is a virtual storm of electrical, magnetic, and chemical activity. This storm of seeming chaotic activity is a big part of what gives us order in our lives. Since the early 1900's scientists and doctors have been able to look into the brain and view this activity, in hopes to decipher why people do one thing verses another. In this project, we tried to solve a part of the puzzle from the view of neuroarchitecture using developing novel high spatial resolution and accurate spatial localization imaging techniques.

Sense organs and the subcortical motor centres provide input to one or more thalamic nuclei, and these nuclei have well-defined reciprocal connections with the cortical regions through which they process sensory information. The reciprocal connections have area and lamina specificity, they are remarkably similar for all cortical areas, and are highly conserved between species. Most of the thalamic input terminates in layer IV of the neocortex, although there are some terminations in layers I, II/III and VI. Layer VI neurons of each area send corticofugal projections back to the corresponding thalamic nucleus, and layer V sends projections to additional nuclei.

The cortical barrels are an orderly organized region in layer IV of rodent primary somatosensory area (SI). Cortical barrels in rodents are specialized functional units corresponding to individual sensory input (1). In the whisker barrel, each barrel contains a cylindrical column of cellular aggregates, approximately 300 – 500 μm in diameter. These barrels are the cortical representation of whiskers; each barrel responds primarily to sensory input from a single whisker. Grid-like arrangement of the cortical barrels has a unique somatotopic representation corresponding to the pattern of whisker arrangement on the contralateral side. In the forepaw barrel subfield, it consists of four bands of barrels, with each corresponds to one digit from the 2nd digit (anterior) to the 5th digit (posterior), that are about 200 – 300 micron in width and 500 – 800 micron in length (1-3). This well-defined relationship between the cortical barrels and the whiskers or forepaw digits makes this system a unique model for the study of neural function and plasticity (3). Therefore, the overall goal of this project is to map the plasticity in layer IV of primary somatosensory cortex of rat brain with high spatial resolution and accurate spatial localization functional imaging methods non-invasively, and to study developmental changes in regional diffusion anisotropy and white matter fiber tract maturation of in vivo rabbit brains with diffusion MRI.

研究目的

The brain is extraordinarily complex, and yet its origin is a simple tubular structure. Characterizing its anatomy at different stages of brain development not only aids in understanding this highly ordered process but also provides clues to detecting abnormalities caused by genetic or environmental factors. The topographic organization of cortical whisker and digit barrels in layer IV of the primary somatosensory cortex (S1) are a well-known example of brain function in rodents. The well-defined relationship between barrels and whiskers/digits makes this system a unique model to study neuronal function and plasticity. The goal of this study was to test the feasibility of manganese-enhanced MRI (MEMRI) and blood oxygenation level dependent (BOLD) functional MRI (fMRI) to map the whisker and forepaw digit representations in the S1 of the rat and its plasticity after digit amputation, and to study developmental changes in regional diffusion anisotropy and white matter fiber tract maturation of in vivo rabbit brains. In this study, we sought to establish a feasible working protocol of applying MEMRI and BOLD fMRI to map the cortical barrels following whisker and digit stimulation and using diffusion MRI to characterize developing rabbit brain.

文獻探討

For centuries, innumerable people have the same dream, which is to understand the relationship between the brain and the body. Many hypotheses and theories have been provided by introspection, behavioral studies, or clinical observations. However, the explanations of the mechanism of how we perceive the outer world, how we do in daily living, how we learn, and so on are far behind the truth. Paul Broca was the first one to show the evidence of language function center in the brain by dissecting the brain of a dead patient who had a lesion in the left frontal area in the late 19th century (4). Later on, more brain functional regions were identified by clinical studies. The exact mechanisms of a normal brain were difficult to be derived from patients due to the complexity of brain lesion sites and symptoms, so a less invasive technique is needed to explore the mystery of a normal brain.

In the 18th century, after knowing that peripheral nerves can transmit messages by electricity, people began to postulate that the brain could also generate electrical signals. People cannot measure the brain neural activity by placing electrodes on the scalp of a normal human subject until early 20th century (5). From that time on, electroencephalogram (EEG) has been widely utilized in the diagnosis and research of spontaneous neural activity. Event-related potential (ERP) techniques have also been invented to observe the activated response time-locked to a specific stimulus. Although both techniques can provide real-time and direct

measurements of neural electrophysiology, the localization capability and the spatial resolution largely limits EEG and ERP in research. In that time, most of our knowledge about brain functions still came from brain lesion studies. Invented in 1972, magnetoencephalography (MEG) can provide a better localization capability, spatial resolution, and complementary information to EEG and ERP (6). However, the complexity on the uncertainty of the inverse problem limit its application to study the interaction between multiple brain regions.

Toward the end of the 19th century, Roy and Sherrington provided the first evidence supporting a coupling between the energy metabolism and the cerebral blood flow (CBF) in the brain (7). In their experiments, a monitoring device was placed on the brain surface of anesthetized dogs, which were measured fluctuations in blood volume. They showed that the blood volume and the presumably flow changed locally in the brain. Brain function could be observed by measuring the hemodynamic or metabolic changes following the neural activity. It was not until 1948 in a seminal experiment measuring oxygen metabolism and blood flow in the brain that Kety and Schmidt confirmed that blood flow in the brain is regionally regulated by the brain itself (8). They demonstrated that when neurons use more oxygen, chemical signals cause the dilation of nearby blood vessels. The increase in vascular volume leads to a local increase in blood flow. At the time of these publications, Kety and Schmidt were considered as vascular physiologists more than brain scientists. Nevertheless the ability to measure CBF, a proven correlate of brain metabolism, opened up the remarkable possibility of studying brain function in humans.

A series of nuclear medicine studies were investigated using positron emission tomography (PET). Several isotopes labeled glucose, water, or dihydroxyphenylalanine (DOPA) were utilized as tracers to map the metabolic rate of glucose, CBF changes, or the activity of a very important neurotransmitter, dopamine, in working human brain (9). Autoradiograph is another radiological image produced on an x-ray film or nuclear emulsion by the pattern of decay emissions from a distribution of a radioactive substance (10). In biology, this technique may be used to determine the tissue localization of a radioactive substance, either introduced into a metabolic pathway, bound to a receptor or enzyme, or hybridized to a nucleic acid. However, the coarse spatial resolution, the slow temporal resolution, and the injection of radioactive tracer are still the limitations for a wide spread application of this technique.

Optical imaging and near infrared spectroscopy (NIRS) are two alternative approaches to measure the hemodynamic response. Optical imaging is a scientific imaging technique using visible or infrared light (11, 12). Optical imaging systems may be divided to the diffusive and ballistic imaging systems. Diffusive optical imaging may give us the ability to simultaneously obtain information about the source of neural activity as

well as its time course (11). Ballistic optical imaging systems ignore the diffused photons and rely only on the ballistic photons to create high-resolution images, near diffraction limit, through scattering media (12). NIRS can map the changes of oxy-hemoglobin and deoxy-hemoglobin in capillaries by recording the reflected infrared signal with very high temporal resolution (13). However, its field of view is limited to a small window on the cortical surface, and its sensitivity depth is also limited compared to tomographic approaches.

In 1991, the cerebral blood volume (CBV) changes under visual stimulation by injecting gadolinium contrast agent were mapped using magnetic resonance imaging (MRI) (14). One year later, Kwong et al. and Ogawa et al. showed that MRI has the capability to map brain function without the need of exogenous contrast agents (15, 16). Functional MRI (fMRI) opened a new era to explore the working human brain. As a brain imaging technique, fMRI has several significant advantages. First, it is non-invasive and does not involve radiation, making it safe for the subjects. Second, it has an excellent spatial and good temporal resolution. Third, it is easy for the experimenters to use.

An alternative function MRI approach is provided by manganese-enhanced MRI (MEMRI), which has the potential to image neural activity by using manganese ion as a MR-detectable contrast agent. Lauterbur first indicates the usefulness of paramagnetic ions for altering contrast (17). Then Lin and Koretsky introduced activity-induced manganese-dependent (AIM) functional MRI technique as an independent surrogate of hemodynamic changes measured in functional MRI using the BOLD mechanism (18). In AIM, the fact that Mn^{2+} ions enter neurons during the stimulation and does not leave rapidly, underlines its unique capability of mapping functioning neurons. Mn^{2+} ions can be injected into animals and taken up by the active neurons in response to the stimulation similar to what they receive from a natural environment, and can be mapped and observed by MRI afterwards (19).

fMRI, MEMRI and diffusion MRI has now been widely used in studying perception, cognitive psychology, psychiatry, brain development, aging, pre-surgical planning, pharmacology, neurology, neural fiber tracking, and plasticity in surgically- or genetically-manipulated rat brains (20). The goal of this project is to map the functional and structural brain in vivo by using these high resolution MR methods non-invasively, and make these techniques becoming more and more reliable and mature in animal studies. In the future, these MRI techniques developed in rats are expected to be extended for use in humans.

研究方法

In diffusion tensor imaging (DTI), data of in vivo rabbit brains (4 weeks to 40 weeks) were acquired and analyzed. Normalized trace apparent diffusion coefficient (ADC), fractional anisotropy (FA), R2 mapping, fiber tracts and voxel sizes were generated and compared across the ages. Our results showed that color maps of diffusion indices, R2 mapping, and 3D tractography revealed that important white matter tracts, such as the olfactory tract, corpus callosum and hippocampus, become apparent during mature period. Regional DTI tractography of the white matter tracts showed refinement in regional tract architecture with maturation. The white matter anisotropy and R2 values increased with age, and the diffusion coefficient decreased with age.

In MEMRI, the protocol was based on the principle of activity-induced manganese-dependent (AIM) contrast. Rats were prepared by sodium pentobarbital anesthetization, intraperitoneal manganese-chloride injection, right common carotid mannitol injection and temperature maintenance. Left whiskers were connected to a speaker through a cotton thread and were stimulated by a series of rectangular pulses. MEMRI was acquired with a 3T scanner 3 h after whisker stimulation. Before MR scanning, Wistar rats were euthanized to avoid motion artifacts. To improve the signal-to-noise ratio (SNR) and detection sensitivity, image coregistration, pixel intensity normalization, statistical mapping, group averaging and subtraction were performed. The AIM enhancement of the cortical barrels was quantified using volume of interest analysis on the acquired T1WI and R1 mapping.

In BOLD fMRI, three dimensional echo-planar imaging with 300 micron isotropic resolution at high field was used to achieve high signal-to-noise ratios and laminar layer resolution. By alternating electrical stimulation of the 2nd (D2) and 4th (D4) digits, functional activation in layer IV of the barrel subfields could be distinguished using a differential analysis. Furthermore, 2 and a half months after the amputation of the 3rd digit in baby rats, the overlapping area between D2 and D4 representations was increased. This indicates that the forepaw barrel subfield previously associated with the ablated digit is now associated with the representation of nearby digits, which is consistent with studies using electrophysiology and cytochrome oxidase staining.

結果與討論

We developed diffusion tensor imaging (DTI) technique for imaging small animal brain (21). We characterized the developmental changes in regional diffusion anisotropy and white matter fiber tract maturation of in vivo developing rabbit brains. Trace apparent diffusion coefficient (ADC), fractional

anisotropy (FA), R2 mapping and fiber tracts were generated and compared across the ages. Our results showed that color maps of diffusion indices, R2 mapping, and 3D tractography revealed that important white matter tracts, such as the olfactory tract, corpus callosum and hippocampus, become apparent during mature period as Fig. 1. Regional DTI tractography of the white matter tracts showed refinement in regional tract architecture with maturation. The white matter anisotropy and R2 values increased with age, and the diffusion coefficient decreased with age. The changes of diffusion indices implied the more restrictive diffusion during mature period. The increases in R2 values reflected the increases of lipids due to the myelination process with maturation. The developing brain DTI database presented can be used for education, as an anatomical research reference, and for data registration. In vivo DTI tractography is potentially a powerful tool for neuroscience investigations.

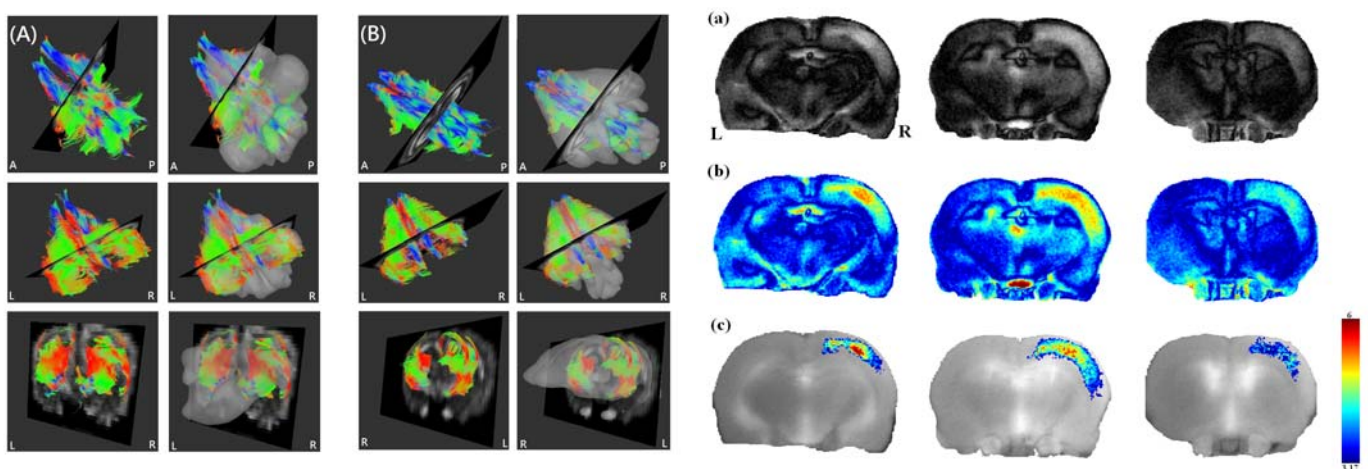


Fig. 1 Whole brain DTI tractography of 4 week-old (a) and 40 week-old (b) rabbits. Three white matter tracts from top row to bottom row were olfactory tracts, corpus callosum and hippocampus, respectively.

Fig. 2. Image subtraction and voxel based t-value mapping between experimental and control groups. The averaged Mn^{2+} -enhanced T1WIs in the control group was subtracted from that in the experimental group. Both gray-level (a) and color (b) maps of the subtracted images and t-value mapping (c) showed that only activity-related right cortical barrels remained enhanced. The threshold of t-value was set to be 3.17 ($p < 0.01$)

Further, we also used topographically organized cortical barrel in layer IV of rat primary somatosensory cortex (S1) as a model for studying neural function and plasticity. To map the brain function and plasticity with high spatial resolution and accurate spatial localization non-invasively, we developed novel imaging techniques and established a feasible working protocol. We successfully apply MEMRI to map the cortical barrels of the rat following whisker stimulation (22). We also tested the feasibility of using BOLD fMRI to map the forepaw digit representations in the primary somatosensory cortex of the rat and to apply to the study of cortical plasticity after digit amputation (23).

In our results, we have mapped rat whisker barrels using the MEMRI method and have shown a clear relationship between manganese-enhanced cortical regions and whisker tactile-sense-evoked activity as Fig. 2. In the right cortical barrels, the enhancement ratios (1.72 ± 0.22) and R1 values (1.12 ± 0.16) in the whisker stimulation group were significantly higher than those (1.27 ± 0.14 , $p < 0.05$; 0.83 ± 0.21 , $p < 0.05$) in the control group. We have also demonstrated that forepaw barrel subfields of single digits can be reliably mapped using fMRI as Fig. 3. The alteration of the digit representation after digit amputation was also detected as Fig. 4. The distance between the centers of mass of two digits representations decreased from 1.45 ± 0.29 mm in the control group to 0.90 ± 0.21 mm ($p < 0.01$) in the amputated group. The method will be useful to study neural plasticity in rat brains after surgical or genetic manipulation. In this research project, the development of these new imaging techniques will be used to study the normal animal brain and changes in the brain that occur during plasticity and rehabilitation due to demyelinating disease.

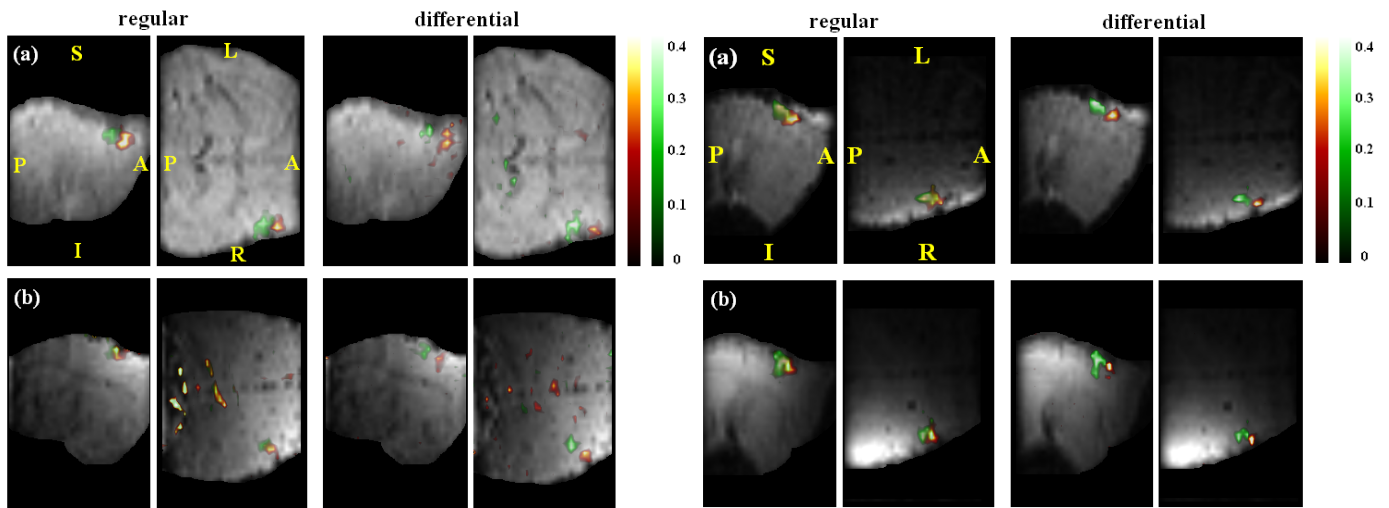


Fig. 3 Functional maps of D2 (red) and D4 (green) in two of the rats (a, b) in the control group created by regular (left column) and differential (right column) analyses. The correlation threshold is 0.2.

Fig. 4 Functional maps of D2 (red) and D4 (green) in two of the rats (a, b) in the amputated group created using the regular (left column) and differential (right column) analyses. The correlation threshold is 0.2.

參考文獻

1. Woolsey TA, Van der Loos H. The structural organization of layer IV in the somatosensory region (SI) of mouse cerebral cortex. The description of a cortical field composed of discrete cytoarchitectonic units. *Brain Res.* 1970;17(2):205-42.
2. Watres R, Li C, McCandlish C. Relationship between the organization of the forepaw barrel subfield and the representation of the forepaw in layer IV of rat somatosensory cortex. *Experimental brain research Experimentelle Hirnforschung.* 1995;103(2):183-97.
3. Welker C. Receptive fields of barrels in the somatosensory neocortex of the rat. *J Comp Neurol.* 1976;166(2):173-89.
4. Broca P. Sur le siege de la faculte du langage articule. *Bull Soc ana de Paris.* 1861;2 Serie(6):355.
5. Orrison W, Lwine J, Sanders J, Hartshorne M. *Functional Brain Mapping.* St. Louis: Mosby-Year Book, Inc.; 1995.
6. Cohen D. Magnetoencephalography: detection of the brain's electrical activity with a superconducting magnetometer. *Science.* 1972;175:664-6.
7. Roy C, Sherrington C. On the regulation of the blood supply of the brain. *J Physiol.* 1890;11:85-108.
8. Kety SS, Schmidt CF. The Nitrous Oxide Method for the Quantitative Determination of Cerebral Blood Flow in Man: Theory, Procedure and Normal Values. *J Clin Invest.* 1948;27(4):476-83.
9. Fox P, Mintun M, Raichle M, Herscovitch P. A noninvasive approach to quantitative functional brain mapping with H₂ 15O and positron emission tomography *J Cereb Blood Flow Metab.* 1984;4:329-33.
10. Yamamura H, Kuhar M, Snyder S. In vivo identification of muscarinic cholinergic receptor binding in rat brain. *Brain Res* 1974; 80(1):170-6.
11. Gibson A, Hebden J, Arridge S. Recent advances in diffuse optical imaging. *Phys Med Biol.* 2005;50:R1-R43.
12. Farsiu S, Christofferson J, Eriksson B, Milanfar P, Friedlander B, Shakouri A, et al. Statistical detection and imaging of objects hidden in turbid media using ballistic photons. *Applied Optics.* 2007;46(23):5805-22.
13. Villringer A, Planck J, Hock C, Schleinkofer L, Dirnagl U. Near infrared spectroscopy (NIRS): a new tool to study hemodynamic changes during activation of brain function in human adults. *Neurosci Lett.* 1993;154:101-4.
14. Belliveau J, Kennedy D, McKinstry R, Buchbinder B, Weisskoff R, Cohen M, et al. Functional mapping of the human visual cortex by magnetic resonance imaging. *Science.* 1991;254:716-9.
15. Kwong K, Belliveau J, Chesler D, Goldberg I, Weisskoff R, Poncelet B, et al. Dynamic magnetic resonance imaging of human brain activity during primary sensory stimulation. *Proc Natl Acad Sci USA.* 1992;89:5951-5.
16. Ogawa S, Tank D, Menon R, Ellermann J, Kim S, Merkle H, et al. Intrinsic signal changes accompanying sensory stimulation: functional brain mapping with magnetic resonance image. *Proc Natl Acad Sci USA.* 1992;89:5951-5.
17. Lauterbur PC. Image Formation by Induced Local Interactions: Examples Employing Nuclear Magnetic Resonance. *Nature* 1973(242):190-1.
18. Lin YJ, Koretsky AP. Manganese ion enhances T1-weighted MRI during brain activation: an approach to direct imaging of brain function. *Magn Reson Med.* 1997;38(3):378-88.

19. Lee JH, Koretsky AP. Manganese enhanced magnetic resonance imaging. *Curr Pharm Biotechnol.* 2004;5(6):529-37.
20. Moonen C, Bandettini P. *Functional MRI.* Berlin: Springer; 1999.
21. Peng Y-W, Wun Y-J, Lai C-H, Weng J-C. In Vivo Characterization of Developing Rabbit Brain with Diffusion Tensor MRI and Tractography. *Proc 19th ISMRM Ann Meeting, Montreal, Quebec, Canada.* 2011:2300.
22. Weng JC, Chen JH, Yang PF, Tseng WY. Functional mapping of rat barrel activation following whisker stimulation using activity-induced manganese-dependent contrast. *Neuroimage.* 2007;36(4):1179-88.
23. Weng JC, Chuang KH, Goloshevsky A, Dodd SJ, Sharer K. Mapping plasticity in the forepaw digit barrel subfield of rat brains using functional MRI. *Neuroimage.* 2011;54(2):1122-9.

國科會補助專題研究計畫項下出席國際學術會議心得報告

日期：100年7月31日

計畫編號	NSC99-2314-B-040-001		
計畫名稱	錳離子增強與擴散磁振造影於大腦功能與軸突纖維束可塑性之研究		
出國人員姓名	翁駿程	服務機構及職稱	中山醫學大學醫學影像暨放射科學系助理教授
會議時間	100年5月7日至 100年5月13日	會議地點	加拿大蒙特婁
會議名稱	(中文)第十九屆國際磁振醫學會 (英文) 19th International Society for Magnetic Resonance in Medicine Annual Meeting		
發表論文題目	(中文) 基於軸突尺寸與密度之q平面磁振造影區分活體大腦胼胝體神經結構 (英文) In Vivo Neuroanatomical Segmentation of Human Corpus Callosum Based on Axonal Diameter and Density Using Q-planar MRI		

一、參加會議經過

今年的國際磁振醫學會(International Society for Magnetic Resonance in Medicine Annual Meeting, ISMRM)於五月7日到13日在加拿大蒙特婁舉行，分為二個部分，包括前二日的 educational courses 及後五日的 scientific meeting，就磁振學會的教育及科學議程內容而言，除生醫應用外，尚且涵蓋磁振造影硬體、波序及基礎研究等這個學門的理論、技術及應用，以口頭或海報發表的研究在量上與北美放射年會(RSNA)幾乎相當，今年共有五千多件研究報告，為歷年之最。其中以「Taiwan」為關鍵字進行光碟檢索或以 PDF 之文字檢索，於 2011 年以台灣之研究或臨床機構名義參與之研究報告有 128 件，佔發表總額之 2.5%，與 2007 年(2.3%，90/3867，本國論文/論文總量)，2005 年(1.6%，57/3661)及 2004 年(1.7%，47/2831)之成果比較，有所進步。另外每天早上都有 morning categorical courses，而傍晚有 study groups，中午及晚上則有磁振造影儀器或藥品等相關的廠商所舉辦的 symposium，所以每天的行程可以說是相當豐富，而也因此學習到不少新知。

二、與會心得

神經塑化(plasticity)是這次會議我關心的重點之一，越來越多的研究團隊以功能性磁振造影(functional MRI)或擴散磁振造影(diffusion MRI)等方法造影神經功能或結構的改變。而擴散除了以前用來觀察神經白質結構之外，現在也有研究團隊克服了許多技術問題，用來觀察灰質結構。擴散磁振造影除了解析神經方向的資訊以外，還有一個重點是顯微結構尺寸的量測，而今年我們所提出的四篇論文中，有二篇與利用擴散磁振造影神經尺寸的量測有關(詳見其他)，不約而同地其他研究團隊也紛紛提出不同的模型來量測神經尺寸，真是百家爭鳴、百花齊放。許多團隊也建立新技術的來改善對比增強磁振造影(contrast enhanced MRI)的品質，並為這個技術找到新的應用。最後，最值得一提是有研究團隊提出磁化率張量造影(susceptibility tensor imaging)的技術，居然利用組織在各個方向磁化率的差異計算出結構的差異，令我非常驚訝與佩服。

三、考察參觀活動(無是項活動者略)

無

四、建議

感謝國科會補助教師出席國際會議發表論文，不啻觀摩並學習他人的研究成果，也藉由教育的課程提昇自己的知識面。這次在加拿大蒙特婁舉辦之 ISMRM 會議提供我們瞭解國際在磁振造影這個領域發展的管道，並且利用出國的機會能與國際上知名的研究團隊討論及交換研究心得，是一個富有研究交流及教育訓練意義的會議。我由衷的建議國內能多鼓勵及補助教師與青年學子參與類似的會議，以達到國內科學的發展及與國際科學的接軌。

五、攜回資料名稱及內容

ISMRM-ESMRMB joint annual meeting 2011 proceeding on DVD

六、其他

1. **Jun-Cheng Weng**, Wen-Yih Isaac Tseng, “In Vivo Neuroanatomical Segmentation of Human Corpus Callosum Based on Axonal Diameter and Density Using Q-planar MRI”, Proc 19th ISMRM Ann Meeting, Montreal, Quebec, Canada, 2011; No. 1994.
2. **Jun-Cheng Weng***, Yeu-Sheng Tyan, “Human Brain Mapping of Orientationally Invariant Axonal Diameter Using Q-space Diffusion Tensor MRI”, Proc 19th ISMRM Ann Meeting, Montreal, Quebec, Canada, 2011; No. 3937.
3. Ling-Yuh Shyu, Hao-Hung Tsai, Shin-Tai Chong, Tzu-Hua Lee, Kwong-Chung Tung, **Jun-Cheng Weng***, “In Vivo Pathological Mapping of the Rat Brain Infected with *Angiostrongylus Cantonensis* using MRI”, Proc 19th ISMRM Ann Meeting, Montreal, Quebec, Canada, 2011; No. 2281.
4. Yi-Wen Peng, Yong-Jheng Wun, Cheng-Hung Lai, **Jun-Cheng Weng***, “In Vivo Characterization of Developing Rabbit Brain with Diffusion Tensor MRI and Tractography”, Proc 19th ISMRM Ann Meeting, Montreal, Quebec, Canada, 2011; No. 2300.

Acceptance

Re: "In Vivo Neuroanatomical Segmentation of Human Corpus Callosum Based on Axonal Diameter and Density Using Q-planar MRI"

Dear Colleague:

Thank you for submitting an abstract to be considered for presentation at the scientific sessions of the ISMRM Annual Meeting in Montréal, Québec, Canada

We are pleased to inform you that your abstract (title above), has been selected for presentation as a traditional poster at this year's Scientific Meeting.

A poster presentation is 60 minutes in length. To maximize opportunities for discussion, one quarter of the posters will be formally presented by authors at each of the four poster sessions. Your poster is assigned to be presented during the following session:

Session: Non-Gaussian Diffusion

Day/Date: Monday, May 9th

Session Start Time: 14:00

Program numbers will be assigned and sent by email within two or three weeks.

Attention Educational and E.K. Zavoisky Stipend Applicants:

Please DO NOT register for the meeting until you have been notified of the status of your stipend application.

Each presenter is assigned a square poster surface which measures 1m/3 ft. 4 in. in height and width. For your convenience, helpful information regarding poster presentations is available at our website. Be sure to monitor the website for current news. Please note that posters must be mounted before 13:00 on Monday, 9 May, and must remain available for viewing until 15:30 on 12 May.

You will be informed of your program number before the meeting. When you arrive at the meeting please verify your program number in the Program in case there have been last minute changes.

The meeting Proceedings will be published on USB drive only, with the full text of all accepted abstracts available to advance registrants online on 23 April. For a list of all abstracts accepted for presentation at the Annual Meeting, please click on: <http://www.ismrm.org/11/abstractresults.pdf>

Please note that, while every effort has been made to honor authors' choices of traditional or e-poster formats, because of thematic or space considerations, some abstracts were not assigned the preferred format. Authors who submitted more than one paper will receive a separate letter indicating the committee's decision on each. On behalf of the Annual Meeting Program Committee, I thank you in advance for your participation in this year's meeting. Our members and attendees look forward to learning about your work.

Best regards,

Caroline Reinhold, Chair
2011 Annual Meeting

In Vivo Neuroanatomical Segmentation of Human Corpus Callosum Based on Axonal Diameter and Density Using Q-planar MRI

J-C. Weng^{1,2}, and W-Y. I. Tseng^{3,4}

¹School of Medical Imaging and Radiological Sciences, Chung Shan Medical University, Taichung, Taiwan, ²Department of Medical Imaging, Chung Shan Medical University Hospital, Taichung, Taiwan, ³Center for Optoelectronic Biomedicine, National Taiwan University College of Medicine, Taipei, Taiwan, ⁴Department of Medical Imaging, National Taiwan University Hospital, Taipei, Taiwan

Introduction

The corpus callosum (CC) is the main fiber tract connecting bilateral cerebral hemispheres, serving information transfer and processing in various cognitive functions. Different CC regions might be affected differently in the development of disease, and their structural parameters such as size and shape might associate with cognitive or functional tests involved in different modes of interhemispheric interactions. Previously we proposed a novel magnetic resonance imaging method called q-planar imaging (QPI), which could in vivo map the relative axonal diameters and density of CC in human brain [1]. We also studied the optimum parameters, cutoff values of diffusion sensitivity b and sampling number, to apply this technique to clinical study [2]. In the study, to further visualize the difference in the computed axonal diameter and density distribution for each voxel, we used cluster analysis to segment the CC based on the QPI parameters, displacement and probability. Correlation analysis was also performed between diffusion spectrum imaging (DSI) and QPI derived parameters. Our cluster results demonstrated that QPI produced reasonable segmentation of relative axonal diameters and density of CC in normal human brain. Poor to moderate correlations between the DSI indices and the parameters derived from QPI implied the incompatibility of the two methods.

Materials and Methods

The CC images in the mid-sagittal plane were acquired from 14 healthy subjects (age: 22-32, M/F: 9/5, all right handedness) using 3T MRI system (Tim Trio, Siemens MAGNETOM, Germany). A multi-slice fast spin echo sequence was performed to obtain T2-weighted (T2W) images with in-plane resolution = 0.55 mm, and slice thickness = 2.5 mm. Images of QPI were acquired using a spin echo diffusion-weighted echo planar imaging (EPI), TR/TE = 1000/142 ms, in-plane resolution = 1.7 mm, slice thickness = 10 mm, and NEX = 1. The diffusion-weighted images were obtained corresponding to 1009 diffusion-encoding directions on a mid-sagittal plane. These encodings directions comprised of isotropic 2D grid points within a round circle of the radius of 18 increments corresponding to b values changing incrementally from 0 to 5000 s/mm². The total scan time for QPI was about 17 minutes.

For QPI data analysis, 2D Fourier transform of signal attenuation in the q-plane was the projected displacement distribution of water molecules inside the tissue [3, 4]. From the full area at half height of displacement distribution, relative axonal diameters of callosal fibers (displacement map) can be acquired. The probability at zero displacement was given by the height of the distribution at zero displacement, which provided information about relative axonal density. The mean square length (MSL) and the diffusion anisotropy (DA) maps were computed from diffusion spectrum imaging (DSI) analysis for comparison. Correlation analysis was also performed between DSI and QPI derived parameters. Specifically, the correlation between probability and DA as well as the correlation between displacement and MSL were analyzed.

To assess the difference between the human CC clusters, k-means analysis was performed. Each pixel in each cluster was regarded as an individual observation. The number of clusters (k) was incremented until no additional information was observed. The final number of clusters was set to six, and one of which was assigned outlier pixels. The data were tested for statistical significance using a repeated measure analysis of variance (ANOVA) with the clusters as the independent factor.

Results and Discussions

To visualize the difference in the computed axonal diameter and density distribution for each voxel, we used cluster analysis to segment the CC based on the QPI parameters, probability and displacement. The analysis results in four different subjects (two male and two female) are shown in Fig. 1. Six clusters were input, one of which represented noise or partial volume at the edges of the CC. The remaining five clusters represented five segments of the structure. In the probability map (Fig. 1a, b, e and f), the red clusters correspond to the genu, the green and blue clusters correspond to the body, the yellow clusters correspond to the isthmus, and the brown cluster corresponds to the splenium. In the displacement map (Fig. 1c, d, g and h), the green clusters correspond to the genu, the red and brown clusters correspond to the body, the yellow clusters correspond to the isthmus, and the blue cluster corresponds to the splenium. Our results showed good agreement with Wiltelson's results in the postmortem morphological study [5]. For the results of correlation analysis (Fig. 2), there was a moderate positive correlation between probability derived from QPI and the DSI index, DA (Fig. 2a), but no significant correlation between displacement and MSL (Fig. 2b). Indeed, the different segments of the CC can be clearly observed in the probability and displacement maps, whereas the segmentation cannot be visualized easily in DA and MSL maps.

Fig. 1 Cluster analysis of the axonal density and diameter distribution along the CC in four different normal subjects. Two are male (a to d) and two are female (e to h). The probability clusters are in the up row (a, b, e and f), and the displacement clusters are in the bottom row (c, d, g and h). Note that the colors of the clusters for the four subjects are matched. Also note the high similarity of the cluster pattern among the subjects.

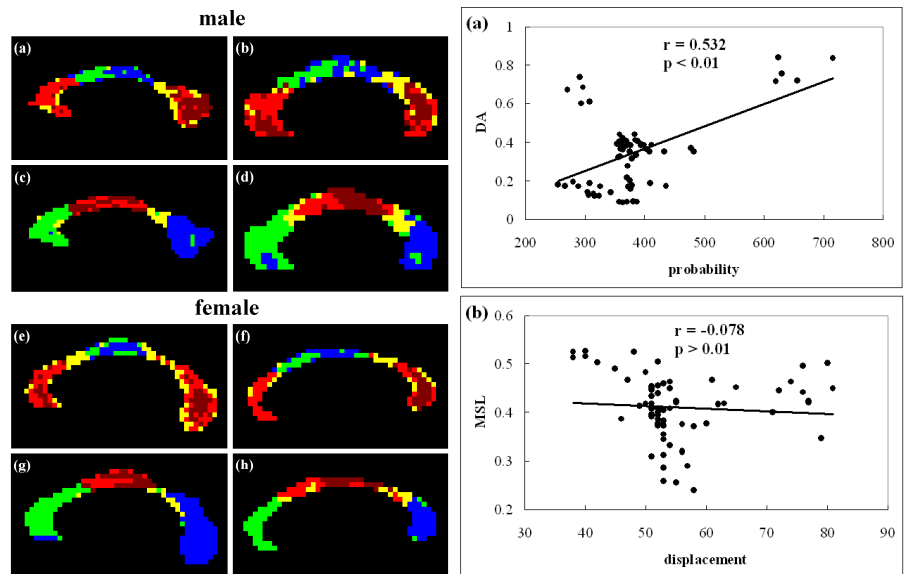


Fig. 2 Comparison of the DSI indices with the indexed QPI maps. (a) Correlation between DA and probability. (b) Correlation between MSL and displacement. Note that the correlations are low to moderate.

Conclusions

We have proposed a QPI method with optimum parameters to map the distribution of relative axonal diameters and density in human CC. The segmentation results based on the QPI-derived parameters are clear and consistent among individuals. Poor to moderate correlations between the DSI indices and the parameters derived from QPI implied the incompatibility of the two methods.

References

- [1] J-C Weng, et al., ISMRM 2010; No. 1562. [2] J-C Weng, et al., OHBM 2010; No. 943. [3] VJ Wedeen, et al., Magn Reson Med 2005; 54: 1377-86. [4] D Barazany, et al., Brain 2009; 132: 1210-20. [5] SF Wiltelson, Brain 1989; 112: 799-835.

Introduction

Fundamental relationships between diffusion tensor imaging (DTI) and q-space imaging can be derived which establish conditions when these two complementary MR methods are equivalent. When the 3D displacement distribution is measured by q-space imaging with large displacement and small q vector, the result is similar to 3D Gaussian assumed in DTI [1]. Combing displacement information from q-space imaging and fiber direction from DTI, distribution of axonal diameters and directions could be derived at the same time. Based on the assumption, the study proposed a novel technique, q-space diffusion tensor imaging (qDTI), to map orientationally invariant axonal diameter distribution of human brain. The goal could be achieved with any of two image reconstruction methods described below. One was tensor-based method. The 3D Gaussian displacement distribution could be obtained directly from the displacement tensor (Fig. 1, bottom row). The other was displacement projection method. The fiber directions were first calculated from conventional DTI, and the mean displacement as well as maximum diffusivity of water molecules along specific direction were then obtained with q-space imaging. The effective axonal diameter was defined as the average of several displacements projected to the direction of the fiber cross section (Fig. 1, right column). Our results demonstrated that two qDTI methods both produced reasonable distribution of orientationally invariant axonal diameters in human brain.

Materials and Methods

The images of human brains were acquired using 3T MRI system (Tim Trio, Siemens MAGNETOM, Germany). A multi-slice spin echo diffusion weighted echo planar imaging (EPI) sequence was performed to obtain qDTI, with TR/TE = 1000/132 ms, in-plane resolution = 2.5 mm, and slice thickness = 10 mm. The diffusion-encoding scheme constituted 24 diffusion-encoding directions with multiple q sampling. Diffusion attenuated images were obtained with diffusion sensitivity (b values) changing from 0 to 5000 s/mm².

For data analysis of q-space imaging, the displacement distribution of water molecules inside the tissue could be obtained by taking Fourier transform of signal attenuation in the q-axis [2]. From the full width at half height of displacement distribution, effective axonal diameters (displacement mapping) could be acquired. The probability at zero displacement was given by the height of the distribution at zero displacement, which provided information reciprocal to the effective axonal diameter [3].

In the tensor-based method, 3D Gaussian displacement distribution could be obtained directly from the displacement tensor (D) as shown in Fig. 2. Eq. (1) was used to calculate the displacement tensor, which was proposed by Basser [1]. The displacement tensor could be obtained using mapping of displacement (r) and probability (P) at zero displacement described above. The eigenvalues and corresponding eigenvectors were then simply derived from the displacement tensor. The orientationally invariant axonal diameter was calculated by the 2nd eigenvalue x 3rd eigenvalue, and the axonal direction was defined as 1st eigenvector.

$$\lim_{r \rightarrow \infty} P(r, \Delta | 0, 0) = \frac{1}{\sqrt{|D|(4\pi\Delta)^3}} e^{-r^T D^{-1} r / (4\Delta)} \tag{1}$$

In the displacement projection method, the axonal direction was first obtained from 1st eigenvector of conventional DTI calculation. Because 24 diffusion-encoding directions with multiple q sampling were acquired, 24 maps of displacement along those diffusion-encoding directions could be calculated as described above. The effective axonal diameter was defined as the average of 24 displacements projected to the plane composed with 2nd and 3rd eigenvectors.

Results and Discussions

Our results showed the reasonable distributions of orientationally invariant axonal diameters of human brain using qDTI technique with tensor-based reconstruction method and displacement projection reconstruction method, respectively (Fig. 3). The yellow color vectors represented the local fiber directions, and the background values reflected the orientationally invariant diameters of these fibers, as indicated by color bar. For example, the main direction of corpus callosum and corticospinal tracts could be obviously observed, and the orientationally invariant axonal diameter of the callosal fibers and corticospinal tracts were smaller than the surrounding tissue.

There were several advantages of the proposed qDTI. The orientationally invariant displacement in each pixel was used to provide novel image contrast indicating axonal diameters. Structural information beyond the spatial resolution of conventional MRI could be inferred without resorting to a complicated tissue model. The novel technique however required a more complicated model in which intracellular and extracellular compartments of specific geometry and exchange between the compartments were taken into consideration.

Fig. 1

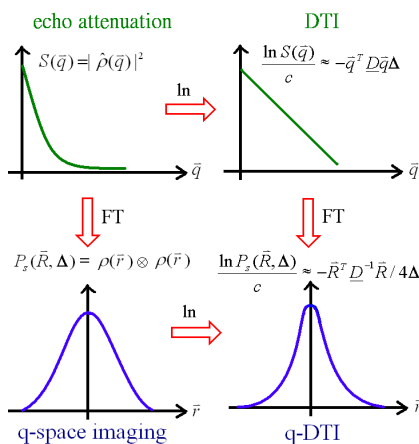


Fig. 2

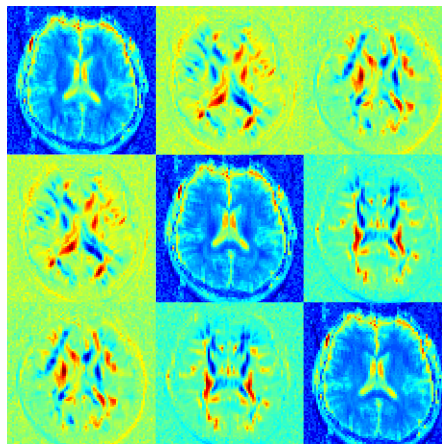


Fig. 3

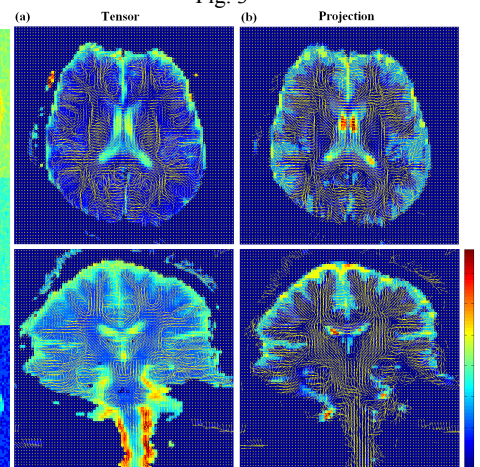


Fig. 1. Fourier and logarithmic relationships among varied diffusion MR imaging methods.

Fig. 2. Displacement tensor elements. Each image responded to one element in the displacement tensor.

Fig. 3. Orientationally invariant axonal diameter mapping of the human brain with (a) tensor-based method and (b) displacement projection method.

Conclusions

Orientationally invariant axonal diameter distribution could be observed in human brain using qDTI. The brain regions might be affected differently in the development of disease, and their structural parameters such as size and shape might associate with cognitive or functional tests involved in different modes of interactions. This technique might be useful in probing the status of myelination in the development of disease.

References

[1] Basser, P.J., MRM 2002; 47(2): 392-397. [2] Wedeen, V.J., MRM 2005; 54(6): 1377-86. [3] Assaf, Y., MRM 2008; 59(6): 1347-54.

Y-W. Peng¹, Y-J. Wun², C-H. Lai¹, and J-C. Weng^{2,3}¹Department of Veterinary Medicine, National Chung Hsing University, Taichung, Taiwan, ²School of Medical Imaging and Radiological Sciences, Chung Shan Medical University, Taichung, Taiwan, ³Department of Medical Imaging, Chung Shan Medical University Hospital, Taichung, Taiwan

Introduction

The brain is extraordinarily complex, and yet its origin is a simple tubular structure. Characterizing its anatomy at different stages of brain development not only aids in understanding this highly ordered process but also provides clues to detecting abnormalities caused by genetic or environmental factors. Diffusion tensor imaging (DTI), a non-invasive method of magnetic resonance imaging (MRI), is sensitive to structural ordering in brain tissue particularly in the white matter tracts. Diffusion anisotropy changes with demyelinating diseases and also with neural development [1, 2]. In the animal studies, however, only ex vivo brains have been studied [3]. Therefore, the goal of this study was to study developmental changes in regional diffusion anisotropy and white matter fiber tract maturation of in vivo rabbit brains. In this study, DTI data of in vivo rabbit brains (4 weeks to 24 weeks) were acquired and analyzed. Normalized trace apparent diffusion coefficient (ADC), generalized fractional anisotropy (GFA), R2 mapping and fiber tracts were generated and compared across the ages. Our results showed that color maps of diffusion indices, R2 mapping, and 3D tractography revealed that important white matter tracts, such as the olfactory tract, corpus callosum and hippocampus, become apparent during mature period. Regional DTI tractography of the white matter tracts showed refinement in regional tract architecture with maturation. The white matter anisotropy and R2 values increased with age, and the diffusion coefficient decreased with age.

Materials and Methods

All images of the whole brain were acquired from five healthy New Zealand rabbits with ages from 4 to 24 weeks using 1.5T MRI scanner (Siemens SONATA, Germany). During MRI experiments, each rabbit was anesthetized with 2-3 % isoflurane mixed with 300 ml/min air using a standard mask (inner diameter = 40 mm, outer diameter = 93 mm), and animal temperature was maintained at ~35.5°C using heat pad. Rabbits were immobilized and double loop array coils were used.

Whole brain T2W images were acquired using turbo spin echo (TSE) sequence with the following parameters: in plane resolution= 0.391×0.781 mm², thickness= 1.5 mm, slice number= 30, repetition time/ echo time (TR/TE)= 3790 ms/ 114 ms, number of excitation (NEX)= 20, and the scan time was about 7 min. For DTI acquisition, whole brain was obtained with two slab scans. For each slab, diffusion weighted images (DWI) were acquired using 2D echo planar imaging (EPI) sequence with the following parameters: in plane resolution= 0.781×0.781 mm², thickness= 2 mm, slice number= 12, TR/TE= 2900 ms/ 133 ms, NEX= 9. The diffusion-encoding scheme constituted 12 diffusion-encoding directions with multiple q sampling. Diffusion attenuated images were obtained with diffusion sensitivity (b values) changing from 0 to 2000 s/mm², and scan time was about 42 min for each slab. To improve detection sensitivity over the full extent of T2 changes during rabbit brain maturation, image data for R2 mapping were acquired. To obtain R2 mapping, single-slice (covering corpus callosum and hippocampus) multi-echo spin echo sequence with the same spatial resolution was performed to acquire 32 sets of images corresponding to 32 different TEs, ranging from 15 to 480 ms, to sample along the decay of transverse magnetization. With NEX= 4, the scan time was about 8 min.

DTI maps and tractography analyses were performed using DSI Studio (National Taiwan University, Taiwan). For tractography, three regions of interest (ROI), olfactory bulbs, corpus callosum and hippocampus, were selected for further analysis. Generalized fractional anisotropy (GFA), normalized trace apparent diffusion coefficient (ADC) and R2 values of these tracts were then calculated. The changes of these diffusion indices across the ages were also compared and discussed.

Results and Discussions

Our results showed that color maps of diffusion indices, R2 mapping (Fig. 1), and 3D tractography (Fig. 2) revealed that important white matter tracts, such as the olfactory tract, corpus callosum and hippocampus, become apparent during mature period (24 weeks). Regional DTI tractography of the white matter tracts showed refinement in regional tract architecture with maturation. There was some minor interanimal tract variability, but there was remarkable similarity between the tracts in all animals. In Fig. 3, the white matter anisotropy and R2 values increased with age, and the diffusion coefficient decreased with age. The changes of diffusion indices implied the more restrictive diffusion during mature period. The increases in R2 values reflected the increases of lipids due to the myelination process with maturation.

Fig. 1

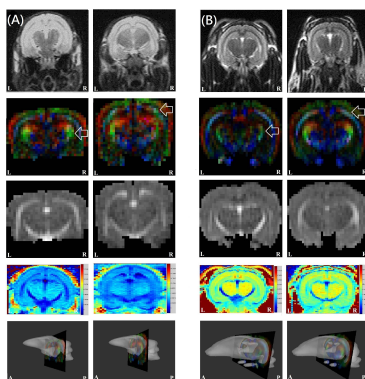


Fig. 1 T2W images, color FA, ACD, R2 mapping and 3D whole brain images of hippocampus (arrow in the left column) and corpus callosum (arrow in the right column) in rabbit brains of 4 weeks old (A) and 24 weeks old (B).

Fig. 2

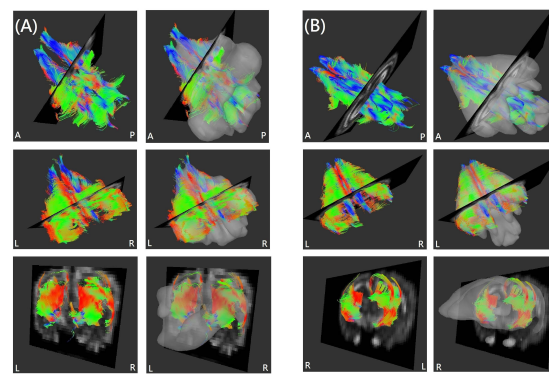
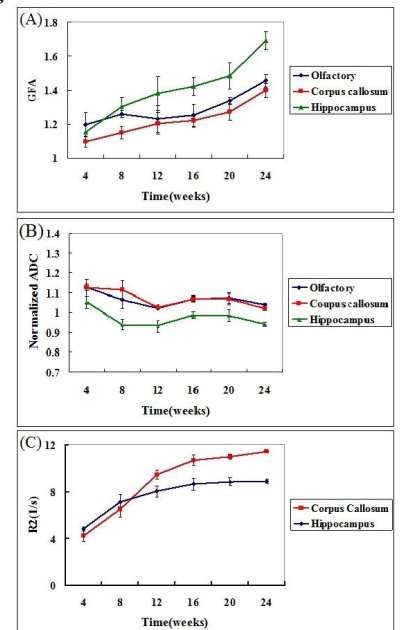


Fig. 2 Whole brain DTI tractography of 4 week-old (A) and 24 week-old (B) rabbit. Three white matter tracts from top row to bottom row were olfactory tracts, corpus callosum and hippocampus, respectively.

Fig. 3 The changes of GFA (A), normalized ADC (B) and R2 value (C) of white matter tracts in the normal rabbits from 4 to 24 weeks.

Fig. 3



Conclusions

The developing brain DTI database presented can be used for education, as an anatomical research reference, and for data registration. In vivo DTI tractography is also a potentially powerful tool for neuroscience investigations and may also reveal effects, such as fiber tract pruning during development, which may be important targets for in vivo human studies.

References

[1] RD Fields, Trends Neurosci 2008; 31: 361-70. [2] P Mukherjee, et al., Neuroimaging Clin N Am 2006; 16: 19- 43. [3] H D'Arceuil, et al., Dev Neurosci 2008; 30: 262-75.

L-Y. Shyu¹, H-H. Tsai^{2,3}, S-T. Chong², T-H. Lee², K-C. Tung⁴, and J-C. Weng^{2,3}¹Department of Parasitology, Chung Shan Medical University, Taichung, Taiwan, ²School of Medical Imaging and Radiological Sciences, Chung Shan Medical University, Taichung, Taiwan, ³Department of Medical Imaging, Chung Shan Medical University Hospital, Taichung, Taiwan, ⁴Department of Veterinary Medicine, National Chung Hsing University, Taichung, Taiwan

Introduction

Angiostrongylus cantonensis (*A. cantonensis*) is the most common cause of eosinophilic meningoencephalitis in Taiwan. This parasitic infection is endemic in the Southeast Asian and Pacific region, but it becomes a global infection in recent years. The infection in the final host, rats, or non-permissive host, including human, is acquired by ingesting contaminated raw snails. The third-stage larvae migrate to the brain and develop into the fifth stage with twice molts. The worms then migrate to lung and heart and develop into adult worm. The typical clinical presentation is acute eosinophilic meningoencephalitis frequently accompanied by brain and spinal cord disorders, and other symptoms of central nervous system (CNS) [1]. The features of the pathological changes in the brain were previously limited to a few case reports and techniques [2, 3]. Previously the diagnosis was established by immunodiagnosis, lumbar puncture and eosinophilia examination. Fourth- or fifth-stage larvae could be found in the cerebrospinal fluid (CSF) with lumbar puncture. Improper puncture and false positive response of immune resulted in an erroneous diagnosis. Therefore, the purpose of this study was to determine the lesion localization, pathological changes and angiostrongyliasis characterization of rat brain infected with larvae of *A. cantonensis* by magnetic resonance imaging (MRI) techniques. The results were verified with histopathological study. Rats were infected with different numbers of *A. cantonensis* larvae and their brains were diagnosed continuously with MRI and histopathological study. The association between the clinical features of the rats and MRI findings was also addressed.

Materials and Methods

In parasite infection, third-stage larvae of *A. cantonensis* were collected from infected *Achatina fulica* snails in Taiping, Taichung, and were isolated by artificial digestion using 0.08% pepsin in 0.7% HCl for 1 hr at 37°C. A total of six male Wistar rats weighing 250 - 300 g (12 weeks old) were used. Three of them were orally inoculated with 100 larvae using a metal feeding tube, and the other three were orally inoculated with 300 larvae, respectively. MR scans were performed before and after infection of *A. cantonensis*. In order to determine the permeability changes of blood-brain barrier after infection, gadodiamide was given by intraperitoneally injecting 151 mg/kg of a 0.5 M Gd-DTPA solution. T1W imaging was performed immediately after T1-shortening contrast agent (gadodiamide) administration. During the MR scanning, the rats were anesthetized with 2% isoflurane mixed with O₂, maintained with 1.5% isoflurane. Rat body temperature was maintained at 37°C using warm water circulation.

The experiment was performed on a 1.5T MRI system (Magnetom Sonata; Siemens Medical Systems, Erlangen, Germany). A surface coil was used for RF reception. Three imaging sequences were performed to acquire whole brain T2 weighted (T2W) images as follows: Multi-slice turbo spin echo (TSE) sequence was performed to obtain T2W images with TR/TE = 3760/114 ms; Fluid attenuation inversion recovery (FLAIR) was performed to obtain T2W images with TR/TE/TI = 8420/155/2500 ms; Half fourier acquisition single shot turbo spin echo (HASTE) was performed to obtain T2W images with TR/TE = 2000/95 ms. All sequences were performed with in-plane resolution = 195µm x 390µm and slice thickness = 1.5 mm. To improve detection sensitivity over the full extent of T2 changes caused by the infection of *A. cantonensis*, image data for R2 mapping were acquired. To obtain R2 mapping, single-slice multi-echo spin echo sequence with half spatial resolution was performed to acquire 32 sets of images corresponding to 32 different TEs, ranging from 15 to 480 ms, to sample along the decay of transverse magnetization. A multi-slice fast spin echo sequence was also performed to obtain contrast-enhanced T1W images in the end of scans with TR/TE = 513/46 ms, in-plane resolution = 195µm x 390µm and slice thickness = 1.5 mm.

Results and Discussions

Abnormal findings on MR images were observed in each rat infected with different numbers of *A. cantonensis* larvae. However, each group of the infected rats with different degrees was found to have variable pathological changes in the brain tissue. In the infection of 100 *A. cantonensis* larvae, hyperintensities near the left and right hippocampus, left and right lateral ventricles, and right dentatus gyrus were found on T2W images of the rat infected after 6 to 28 days (Fig. 1a - 1c, 1e). In the same period, the contrast-enhanced T1W images after intravenous administration of gadolinium showed hypointensities without enhancement near the left and right hippocampus, left and right lateral ventricles and right tractus (Fig. 1d). Both T2W and contrast-enhanced T1W images showed hyperintensities in subarachnoid space of the rat brain infected after 20 to 28 days (Fig. 1). In the infection of 300 *A. cantonensis* larvae, T2W and contrast-enhanced T1W images showed more obvious hyperintensities and hypointensities in the same areas of the rat brains (than infection of 100 larvae) infected after 4 to 24 days (Fig. 2). T2W and contrast-enhanced T1W images both showed hyperintensities in subarachnoid space of the rat brain infected after 14 to 24 days (Fig. 2). Our MR results were consistent with histopathological study. Moreover, fifth-stage larvae of *A. cantonensis* in the brain parenchyma near subarachnoid space were found in most rats (Fig. 3).

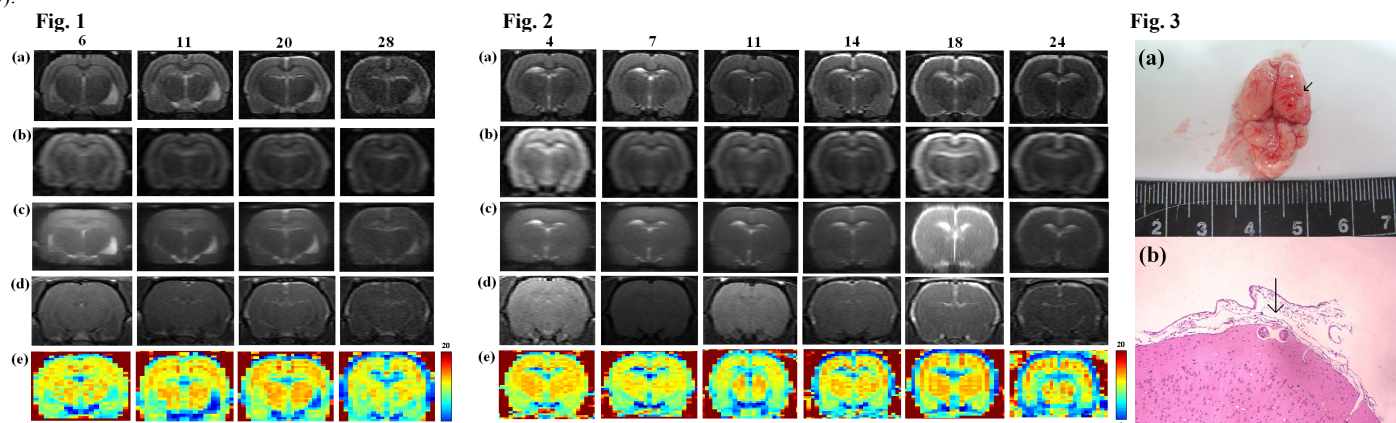


Fig. 1 (a) T2W images, (b) FLAIR, (c) HASTE, (d) contrast-enhanced T1W images and (e) R2 mapping of rat brains infected with 100 *A. Cantonensis* larvae after 6, 11, 20 and 28 days infection, respectively.

Fig. 2 (a) T2W images, (b) FLAIR, (c) HASTE, (d) contrast-enhanced T1W images and (e) R2 mapping of rat brains infected with 300 *A. Cantonensis* larvae after 4, 7, 11, 14, 18 and 24 days infection, respectively.

Fig. 3 (a) Photograph and (b) microphotograph of histopathology showed a fifth-stage larva in the brain parenchyma near subarachnoid space (arrow).

Conclusions

Our MRI results showed pathological changes in the rat brains infected with 300 *A. cantonensis* larvae were more severe than those infected with 100 *A. cantonensis* larvae. MRI was sensitive in showing tissue change and oedema, and provided higher tissue contrast and superior sensitivity in the detection of lesions. Therefore, MRI was suggested to be a non-invasive technique in localizing and characterizing lesions during the acute phase of angiostrongyliasis due to *A. cantonensis*.

References

[1] Alicata JE. *Advances in Parasitology*, 1965; 3: 223-248. [2] Tsai H-C., et al., *Am. J. Trop. Med. Hyg.*, 2003; 68(3): 281-285. [3] Wang L-C., et al., *J Antimicrob Chemother*, 2006; 57: 294-300.

國科會補助計畫衍生研發成果推廣資料表

日期:2011/10/25

國科會補助計畫	計畫名稱: 錳離子增強與擴散磁振造影於大腦功能與軸突纖維束可塑性之研究
	計畫主持人: 翁駿程
	計畫編號: 99-2314-B-040-001- 學門領域: 放射線及核子醫學
無研發成果推廣資料	

99 年度專題研究計畫研究成果彙整表

計畫主持人：翁駿程		計畫編號：99-2314-B-040-001-				計畫名稱：錳離子增強與擴散磁振造影於大腦功能與軸突纖維束可塑性之研究	
成果項目		量化			單位	備註（質化說明：如數個計畫共同成果、成果列為該期刊之封面故事...等）	
		實際已達成數（被接受或已發表）	預期總達成數（含實際已達成數）	本計畫實際貢獻百分比			
國內	論文著作	期刊論文	0	0	100%	篇	為二個計畫共同成果
		研究報告/技術報告	0	0	100%		
		研討會論文	19	0	90%		
		專書	0	0	100%		
	專利	申請中件數	0	0	100%	件	
		已獲得件數	0	0	100%		
	技術移轉	件數	0	0	100%	件	
		權利金	0	0	100%	千元	
	參與計畫人力（本國籍）	碩士生	3	0	80%	人次	
		博士生	0	0	100%		
博士後研究員		0	0	100%			
專任助理		0	0	100%			
國外	論文著作	期刊論文	2	0	90%	篇	為二個計畫共同成果
		研究報告/技術報告	0	0	100%		
		研討會論文	11	0	90%		
		專書	0	0	100%		
	專利	申請中件數	0	0	100%	件	
		已獲得件數	0	0	100%		
	技術移轉	件數	0	0	100%	件	
		權利金	0	0	100%	千元	
	參與計畫人力（外國籍）	碩士生	3	0	80%	人次	
		博士生	0	0	100%		
博士後研究員		0	0	100%			
專任助理		0	0	100%			

<p>其他成果 (無法以量化表達之成果如辦理學術活動、獲得獎項、重要國際合作、研究成果國際影響力及其他協助產業技術發展之具體效益事項等，請以文字敘述填列。)</p>	<p>後學獲得下列獎勵，指導四位學生獲得國內研討會論文獎。 九十八學年度中山醫學大學醫學影像暨放射科學系研究績優獎 九十九學年度第二學期中山醫大教師研究論文發表獎勵 九十九學年度中山醫學大學醫學科技學院教學特優教師</p>
--	---

	成果項目	量化	名稱或內容性質簡述
科 教 處 計 畫 加 填 項 目	測驗工具(含質性與量性)	0	
	課程/模組	0	
	電腦及網路系統或工具	0	
	教材	0	
	舉辦之活動/競賽	0	
	研討會/工作坊	0	
	電子報、網站	0	
	計畫成果推廣之參與(閱聽)人數	0	

國科會補助專題研究計畫成果報告自評表

請就研究內容與原計畫相符程度、達成預期目標情況、研究成果之學術或應用價值（簡要敘述成果所代表之意義、價值、影響或進一步發展之可能性）、是否適合在學術期刊發表或申請專利、主要發現或其他有關價值等，作一綜合評估。

1. 請就研究內容與原計畫相符程度、達成預期目標情況作一綜合評估

達成目標

未達成目標（請說明，以 100 字為限）

實驗失敗

因故實驗中斷

其他原因

說明：

2. 研究成果在學術期刊發表或申請專利等情形：

論文： 已發表 未發表之文稿 撰寫中 無

專利： 已獲得 申請中 無

技轉： 已技轉 洽談中 無

其他：（以 100 字為限）

3. 請依學術成就、技術創新、社會影響等方面，評估研究成果之學術或應用價值（簡要敘述成果所代表之意義、價值、影響或進一步發展之可能性）（以 500 字為限）

我們成功的建立錳離子增強磁振造影、擴散磁振造影、與功能性磁振造影於小動物功能與神經結構迴路的實驗與分析平台，並用於研究大鼠大腦功能區塑化與大白兔大腦主要神經發育的情形。而此平台的建立是相當具有前瞻性的醫學研究，以及臨床應用與醫療市場產業價值。我們的研究結果也發表三篇國際期刊論文，以及數篇國內外研討會論文。這些成果對於腦神經科學研究、精神醫學研究、結構性與功能性磁振造影等科學具有所參考價值，並可提高本校與本院醫學研究水準。參與研究之人員可學習磁振造影系統基礎理論、技術、影像分析之能力，以及研發新的造影技術，瞭解建立平台時所面臨之問題，培養解決問題的能力，這些訓練對於從事醫學影像研究者而言非常重要。並藉由本實驗學習結構性與功能性磁振造影的操作與分析，並可將這些相關技術應用在其它疾病的磁振造影的研究，同時了解一個研究計畫的執行過程以及如何將實驗成果做到最有價值的運用。未來可將此分析平台應用於評估腦部其它去髓鞘變化後可能的大腦皮質活化區塊與迴路狀態的改變，幫助相關疾病進展與治療前後的評估，並且可進一步探索或研發相關技術與醫儀器材，進而提升國內醫療品質、民眾福祉與醫療相關研究之發展。